ORIGINAL ARTICLE

Left ventricular strain-curve morphology to distinguish between constrictive pericarditis and restrictive cardiomyopathy

Zhiyun Yang[1] (iD), Hui Wang[2], Sanshuai Chang[1], Jing Cui[1], Lu Zhou[1], Qiang Lv[1], Yi He[3], Xin Du[1], Jianzeng Dong[1,4]* and Changsheng Ma[1]

[1]Department of Cardiology, Beijing Anzhen Hospital, Capital Medical University, National Clinical Research Center for Cardiovascular Diseases, Beijing, China; [2]Department of Radiology, Beijing Anzhen Hospital, Capital Medical University, Beijing, China; [3]Department of Radiology, Beijing Friendship Hospital, Capital Medical University, Beijing, China; and [4]Department of Cardiology, the First Affiliated Hospital, Zhengzhou University, Zhengzhou, 450052, China

Abstract

Aims   To distinguish between constrictive pericarditis (CP) and restrictive cardiomyopathy (RCM) using cardiac magnetic resonance feature tracking (CMR-FT) left ventricle (LV) diastolic time–strain curve patterns and myocardial strain.
Methods and Results   A total of 32 CP patients, 27 RCM patients, and 25 control subjects were examined by CMR-FT and analysed for global strain, segmental strain, and LV time–strain curve patterns in the longitudinal, circumferential, and radial directions. Speckle tracking echocardiography (STE) strain imaging was performed in some cases. The peak global longitudinal strain (GLS) and global circumferential strain (GCS) of the RCM group were lower than those of the CP group. GLS [median (interquartile range) CP vs. RCM: −11.15 (−12.85, −9.35) vs. −6.5 (−8.75, −4.85), $P < 0.001$] and GCS (CP vs. RCM: −16.89 ± 5.11 vs. −13.37 ± 5.79, $P < 0.001$). In circumferential and radial directions, the strain ratios of the LV lateral/septal wall (LW/SW) of the CP group were significantly lower than those of the RCM group at the basal and mid segments. The CS ratio of LW/SW at the basal segment [CP vs. RCM: 0.95 (0.85, 1.25) vs. 1.43 (1.18, 1.89), $P < 0.001$] and mid segment [CP vs. RCM: 1.05 (0.92, 1.15) vs. 1.18 (1.06, 1.49), $P = 0.026$]. The RS ratio of LW/SW at the basal segment [CP vs. RCM: 0.97 (0.76, 1.37) vs. 1.55 (1.08, 2.31), $P = 0.006$] and mid segment [CP vs. RCM: 0.95 (0.70, 1.28) vs. 1.79 (1.32, 2.92), $P < 0.001$]. In the longitudinal and circumferential directions, the characteristic 'plateau' pattern of time–strain curves could be seen in the CP but not in the RCM during the diastole. The GCS ratio of 0–50%/50–75% diastolic period of the CP was higher than that of the RCM [CP vs. RCM: 17.01 (8.67, 23.75) vs. 5.38 (1.93, 11.24), $P = 0.001$], while the GCS ratio of 50–75%/75–100% diastolic period was lower than that of the RCM [CP vs. RCM: 0.36 (0.15, 1.67) vs. 1.12 (0.70, 5.58), $P < 0.001$]. The peak GLS (sensitivity, 85%; specificity, 78%) and the GCS ratio of 0–50%/50–75% diastolic period (sensitivity, 88%; specificity, 73%) had higher differential diagnosis value.
Conclusions   The CMR-FT could distinctly differentiate CP from RCM based on LV myocardial strain and LV time–strain curve patterns. The characteristic 'plateau' pattern of the time–strain curve is specific for CP and not RCM and this curve can also be duplicated by STE.

Introduction

Both constrictive pericarditis (CP) with restraint of pericardium and restrictive cardiomyopathy (RCM) with increased stiffness of the myocardium have similar cardiac structural features that are characterized by normal-sized ventricles and dilated atria.[1,2] Moreover, CP and RCM also have similar clinical characteristics such as elevated left ventricular end-diastolic pressure, prolonged ventricular relaxation, impaired diastolic filling, and retained systolic function,[3] all of

which manifest as abnormalities of diastolic function and further present as heart failure with preserved ejection fraction. Conversely, the surgical indication and prognosis of CP and RCM are very different. Patients with CP after pericardiectomy have a prognosis with survival rates of ≥80% at 5–7 years.[4] However, the therapeutic options for RCM are very limited and the prognosis is usually poor; understandably, surgery for RCM that is misdiagnosed as CP can have catastrophic consequences.[5] At present, the conventional methods for differentiation of CP and RCM are as follows: echocardiography (respiratory-related ventricular septal shift in CP);[6,7] chest computed tomography (CT, thickening of the pericardium [>4 mm]);[8] and cardiac magnetic resonance (CMR) imaging examination including T2 relaxation time sequences, short-tau inversion-recovery sequences, and late gadolinium enhancement.[9] The conventional imaging methods may lead to misdiagnosis and cannot completely distinguish CP and RCM.[10] Hence, more distinct diagnostic criteria are necessary.

In RCM, abnormal fibrosis and necrosis of the myocardium cause diastolic dysfunction and continuous damage to the cardiac process from early diastole to end diastole. CP is inhibited by external pericardial restraint and retained parts of normal myocardial relaxation function in the early diastole. Therefore, there is a significant difference in the diastolic process between CP and RCM. Myocardial tissue tracking imaging such as CMR feature tracking (CMR-FT) and speckle-tracking echocardiography (STE) have been used as non-invasive assessments of myocardial deformation and provide a way to distinguish CP from RCM. However, previous studies on the distinction between CP and RCM only focused on one aspect of the peak global strain and segmental myocardial strain of the left ventricle (LV) wall, thereby lacking a comprehensive and systematic study of the LV myocardial deformation.[11–13] Furthermore, the imaging of LV diastolic function in CP and RCM remains incompletely understood. Hence, in our study, we emphasized evaluating peak global longitudinal strain (GLS), global circumferential strain (GCS), global radial strain (GRS), and the strain ratio of LV lateral/septal wall (LW/SW) at different segments to quantify LV global and segmental myocardial deformation in CP and RCM. Furthermore, we also noticed different morphologies of LV characteristic time–strain curve patterns that could reflect the differences in the diastolic process and haemodynamic characteristics of these two diseases.

Methods

## Population and study protocol

In this retrospective study, from January 2014 to November 2020, all patients who underwent echocardiography and CMR examination at Anzhen Hospital (Capital Medical University of Beijing, China) and were diagnosed with CP and RCM were enrolled. Age-matched and sex-matched healthy volunteers were included as control subjects with no history of cardiovascular disease, and who showed essentially normal cardiac structure and function on echocardiography and CMR. The diagnosis of CP was made according to surgical pericardiectomy or all of the following additional criteria: (i) evidence of thickened pericardium (thickness >4 mm by CT, echocardiography, or CMR) and (ii) evidence of increased LV-RV coupling (septal shift with respiration) by echocardiography or CMR.[14,15] The diagnosis of RCM was based on a biopsy of the heart, kidney, or other organs that had been confirmed as amyloidosis, or all of the following echocardiographic and CMR features: (i) a hypertrophic interventricular septum >12 mm; (ii) preserved ejection fraction > 50%; (3) bilateral atrium enlargement; (4) restrictive filling pattern, as well as evidence of myocardial involvement in delayed gadolinium-enhanced CMR[11] (*Figure 1*). All CP and RCM patients and healthy volunteers had sinus rhythm. Valvular heart disease, arrhythmia, myocardial infarction, hypertension, and other causes of myocardial hypertrophy and dysfunction were excluded from this study.

The study protocol was approved by the Institutional Ethics Committee of Anzhen Hospital, Capital Medical University of Beijing, China (Approval No.: 2006003x). Written informed consent was obtained from all study participants.

Echocardiographic measurements and strain analysis by speckle-tracking echocardiography

All patients underwent comprehensive 2D echocardiogram and Doppler evaluations using the Philips IE33 system (Philips Medical Systems, Acuson 512; Andover, MA, USA), which were performed and interpreted according to the American Society of Echocardiography Guidelines.[16] LV end-diastolic diameter (LVEDD), LV end-systolic diameter (LVESD), LV ejection fraction (LVEF), and LV septal wall thickness were calculated according to the biplane modified Simpson method in the apical two-chamber and four-chamber views. The mitral inflow velocities were evaluated by pulsed Doppler echocardiography. The peak filling velocity of early (E wave), late (A wave), and mitral annular early diastolic velocity (e′) were measured. The E/A wave and E/e′ ratio were calculated. Patients with CP and RCM who were diagnosed and included in this study from April 2020 underwent LV-STE assessment using 2D-STE software (QLAB; Philips Healthcare). The global longitudinal strain and pattern of strain curve were computed by two-chamber, three-chamber, and four-chamber views.

Figure 1 Subject selection of inclusion and exclusion criteria. CP, constrictive pericarditis; RCM, restrictive cardiomyopathy.
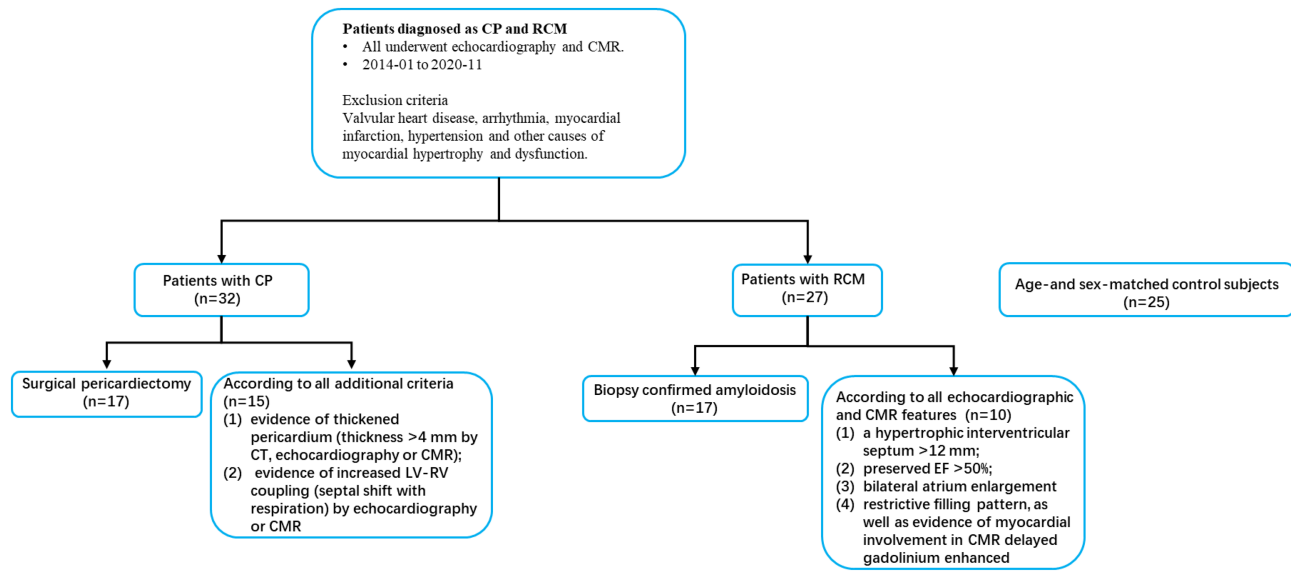
Cardiac magnetic resonance data acquisition and strain analysis by cardiac magnetic resonance feature tracking

All subjects underwent a standardized CMR myocardial function study on a 3.0 T Siemens scanner (Magnetom Verio; Siemens AG Healthcare, Erlangen, Germany) and a 3.0T GE scanner (Discover MR750W). Cine images in contiguous short axis slices covered the whole ventricles from the annulus of the AV valves to the apex, with 25 phases per cardiac cycle. Long-axis cine single shot fast precession images, rest myocardial perfusion, and late enhanced images using gadolinium were acquired for assessment of myocardial function. All analyses were performed on a commercially available workstation with CVI42 software (version 5.11.3, Circle Cardiovascular Imaging). Endocardial and epicardial contours were traced by CVI42 in the end-diastolic and end systolic phases with manual calibrations, if needed. The LV end-diastolic volume (LVEDV), LV end-systolic volume (LVESV), LVEF, and myocardial mass (diastolic) were computed automatically after the endocardial and epicardial borders were drawn. Three-dimensional feature tracking was used for semi-automated analysis for GLS, GCS, GRS, the global strain ratio of LW/SW, and LV characteristic time–strain curve patterns. Both CMRFT and LV-STE were performed before or without pericardiectomy in CP patients.

Statistical analysis

Continuous variables are expressed as mean ± SD or median (interquartile range), and categorical variables are expressed as numbers (*n*) and percentages. For normally distributed continuous variables, analysis of variance (ANOVA) with Tukey's adjustment for multiple comparisons assessed the differences between each group. For non-normally distributed variables, the Kruskal–Wallis test was used. Categorical variables were tested by χ^2 or Fisher's exact tests. Receiver operating characteristic curve analysis was used to evaluate the sensitivity and specificity of various CMR-FT parameters to distinguish CP from RCM. $P < 0.05$ was considered to indicate statistical significance. All analyses were performed using the SPSS statistical software (SPSS software version 22.0, IBM Corporation, Armonk, NY, USA).

Results

A total of 32 CP patients, 27 RCM patients, and 25 control subjects were included in our study (*Figure 1*). In the CP group, 17 patients (53%) underwent pericardiectomy, of which 13 also met the criteria of imaging examination. The remaining 15 patients (47%) were confirmed by CT, echocardiography, and CMR. In the RCM group, 10 patients (37%) had cardiac or extracardiac biopsy proven amyloidosis, of which eight also met the imaging criteria. The remaining 17 patients (63%) showed a restrictive filling pattern, which had myocardial infiltration, subendocardial delayed gadolinium enhancement, and fibrosis confirmed in the CMR.

Baseline clinical characteristics

Table 1 summarizes the clinical characteristics and echocardiographic and CMR measurements of the three groups. CP patients had higher heart rates than the control group

Table 1 Clinical characteristics

	CP (n = 32)	RCM (n = 27)	Control (n = 25)	F/H/χ^2 value	P value
Age, years	49.5 (35.0, 58.5)	57.0 (43.0, 66.5)	36.5 (30.8, 47.8)	5.320	0.070
Male sex, n (%)	21 (65.6)	22 (81.5)	12 (48.0)	6.438	0.050
Height, cm	168.6 ± 7.5	168.2 ± 9.5	163.8 ± 5.8	1.472	0.239
Weight, kg	65.0 (59.0, 80.5)	40.0 (38.0, 47.5)	72.5 (64. 0, 80.0)	3.065	0.216
BSA, cm/m^2	1.76 ± 0.21	1.85 ± 0.25	1.72 ± 0.17	1.443	0.246
BMI, kg/m^2	23.8 ± 3.5	26.0 ± 4.8	24.3 ± 3.0	1.857	0.166
Heart rate, bpm	86.7 (72.6, 95.1)[†]	80.0 (68.4, 87.4)	74.5 (72.3, 90.8)	12.065	0.002
Echocardiogram					
LV septum, mm	8.5 ± 1.5[#]	12.9 ± 3.8*	8.2 ± 1.1	21.313	<0.001
LVEDD, mm	41.0 (38.0, 47.5)	44.0 (41.0, 51.5)	43.5 (38.0, 47.0)	4.193	0.123
LVEDS, mm	26.0 (24.0, 32.5)[#]	32.0 (28.0, 37.5)	27.5 (26.5, 29.8)	8.909	0.012
LVEF, %	61.2 ± 7.4[†,#]	52.4 ± 13.3*	67.1 ± 2.4	8.833	<0.001
E wave, m/s	85.0 ± 23.0	81.8 ± 37.8	88.8 ± 10.3	0.194	0.824
A wave, m/s	49.0 (37.5, 68.0)	63.0 (44.0, 84.5)	62.0 (56.8, 77.3)	2.026	0.363
E/A wave	1.5 (1.1, 2.0)	1.0 (0.8, 1.4)	1.5 (1.3, 1.6)	4.921	0.085
e/, cm/s	8.5 (8.0, 12.1)	6.2 (5.1, 7.6)	7.4 (6.1, 9.8)	3.370	0.050
E/e/	9.9 (9.0, 13.3)	13.4 (10.8, 18.6)	9.4 (8.2, 11.8)	1.438	0.237
CMR					
LVEDV, mL	94.3 (78.6, 137.4)	117.3 (68.5, 156.0)	114.7 (87.8, 126.3)	3.412	0.182
LVESV, mL	44.9 (32.7, 67.1)	52.3 (34.8, 93.4)	43.0 (24.1, 48.5)	3.698	0.157
LVEF, %	50.7 ± 11.6 [†,#]	43.4 ± 14.7*	63.4 ± 6.6	19.758	<0.001
Myo mass, g	66.4 (56.9, 98.2)[#]	120.0 (99.6, 189.2)	77.1 (63.4, 106.0)	11.929	0.003
Myocardial enhancement, n (%)	1 (3.1)	21 (77.8)	…		…

BMI, body mass index; BSA, body surface area; CP, constrictive pericarditis; EDD, end-diastolic diameter; EDV, end-diastolic volume; EF, ejection fraction; ESD, end systolic diameter; ESV, end systolic volume; LV, left ventricle; Myo mass, myocardial mass (diastolic); myocardial enhancement, focal enhancement in CP patients, and diffuse enhancement in RCM patients; RCM, restrictive cardiomyopathy.
Continuous variables are presented as mean ± SD or median (interquartile range) and categorical variables as numbers (n) and percentages.
[#]$P < 0.05$ CP vs. RCM.
[†]$P < 0.05$ CP vs. control.
*$P < 0.05$ RCM vs. control.

($P < 0.05$). There were no significant differences in age, sex, height, weight, BSA, and BMI among the CP, RCM, and control groups. The results of echocardiography showed that the LV wall thickness and LV end-systolic diameter of RCM patients were higher than those of CP patients ($P < 0.05$), while the LVEF was lower than that of CP patients ($P < 0.05$). There were no significant differences in E/A wave and E/e/ ratio between CP and RCM. CMR measurements showed that RCM had higher myocardial mass and lower LVEF than CP ($P < 0.05$).

Peak global strain and the strain ratio of lateral/septal wall

The peak GLS and GCS of the RCM group were lower than those of the CP group and control group. GLS [CP vs. RCM: −11.15 (−12.85, −9.35) vs. −6.5 (−8.75, −4.85), $P < 0.001$] and GCS (CP vs. RCM: −16.89 ± 5.11 vs. −13.37 ± 5.79, $P < 0.001$). While the peak GRS in the CP and RCM groups were lower than those in the control group, but there was no significant difference in peak GRS between the CP and RCM groups (*Table 2*). *Table 2* also shows the strain ratios of LV lateral/septal wall (LW/SW) of CP and RCM in different directions and different segments. In longitudinal directions, the strain ratios of LW/SW of CP and

RCM had no significant difference in the basal, mid, and apical segments. In circumferential and radial directions, the strain ratios of LW/SW of the CP group were significantly lower than that of the RCM group at the basal and mid segments. The CS ratio of LW/SW at the basal segment [CP vs. RCM: 0.95 (0.85, 1.25) vs. 1.43 (1.18, 1.89), $P < 0.001$] and mid segment [CP vs. RCM: 1.05 (0.92, 1.15) vs. 1.18 (1.06, 1.49), $P = 0.026$]. The RS ratio of LW/SW at the basal segment [CP vs. RCM: 0.97 (0.76, 1.37) vs. 1.55 (1.08, 2.31), $P = 0.006$] and mid segment [CP vs. RCM: 0.95 (0.70, 1.28) vs. 1.79 (1.32, 2.92), $P < 0.001$], whereas there was no significant difference between the two groups in the apical segment.

Left ventricle time–strain curve patterns

As shown in *Figure 2*, the global time–strain curves of every subject derived by CMR-FT were normalized using the two reference time points of end-diastole and next end-diastole; therefore, that time was expressed as a percentage of time (% heartbeat cycle length) and then averaged to a total time–strain curve pattern of different groups in different directions (with error bars indicating standard deviation). A total of three different diastolic patterns corresponding to the average time–strain curves were identified in patients with CP, RCM, and the controls in the longitudinal and

Table 2 Peak global strain and the strain ratio of LV lateral/septal wall

|	CP ($n = 32$)	RCM ($n = 27$)	Control ($n = 25$)	F/H value	P value
Peak GLS (%)	−11.15 (−12.85, −9.35)[#,†]	−6.5 (−8.75, −4.85)[*]	−15.21 (−16.83, −11.97)	32.412	<0.001
Peak GCS (%)	−16.89 ± 5.11[#,†]	−13.37 ± 5.79[*]	−23.40 ± 2.27	30.058	<0.001
Peak GRS (%)	30.60 (19.80, 35.70)[†]	17.10 (10.90, 31.00)[*]	43.49 (35.49, 51.01)	27.981	<0.001
LS ratio of LW/SW					
Basal	1.02 (0.84, 1.31)	0.94 (0.74, 1.16)	0.99 (0.83, 1.07)	2.156	0.340
Mid	0.94 (0.85, 0.99)	0.99 (0.76, 1.30)	0.98 (0.87, 1,08)	2.124	0.346
Apical	1.02 (0.86, 1.18)	1.22 (1.00, 1.38)	1.23 (1.05, 1.34)	6.680	0.035
CS ratio of LW/SW					
Basal	0.95 (0.85, 1.25)[#]	1.43 (1.18, 1.89)	1.18 (1.13, 1.27)	14.987	0.001
Mid	1.05 (0.92, 1.15)[#]	1.18 (1.06, 1.49)	1.08 (0.95, 1.18)	7.511	0.023
Apical	1.10 (0.91, 1.31)	1.17 (0.87, 1.50)	1.07 (1.01, 1.17)	0.873	0.646
RS ratio of LW/SW					
Basal	0.97 (0.76, 1.37)[#]	1.55 (1.08, 2.31)	1.12 (0.88, 1.50)	9.770	0.008
Mid	0.95 (0.70, 1.28)[#]	1.79 (1.32, 2.92)	1.27 (1.02, 1.67)	22.505	<0.001
Apical	1.11 (0.83, 1.50)	1.26 (0.88, 1.74)	1.33 (0.92, 1.61)	0.456	0.796

CP, constrictive pericarditis; CS, circumferential strain; GCS global circumferential strain; GLS, global longitudinal strain; GRS, global radial strain; LS, longitudinal strain; LW/SW, lateral/septal wall; RCM, restrictive cardiomyopathy; RS, radial strain.
Continuous variables are presented as mean ± SD or median (interquartile range).
[#]$P < 0.05$ CP vs. RCM.
[†]$P < 0.05$ CP vs. control.
[*]$P < 0.05$ RCM vs. control.

Figure 2 LV time -strain curve patterns of the CP, RCM, and control groups. The CP (red line), RCM (yellow line), and control (blue line) groups are presented with mean and error bars (mean ± SD) in the longitudinal, circumferential, and radial directions and normalized for the duration of the cardiac cycle. The duration of the cardiac cycle refers to the time from the end-diastole to the next end-diastole. CP, constrictive pericarditis; RCM, restrictive cardiomyopathy; GLS, global longitudinal strain; GCS global circumferential strain; GRS, global radial strain; LV, left ventricle.
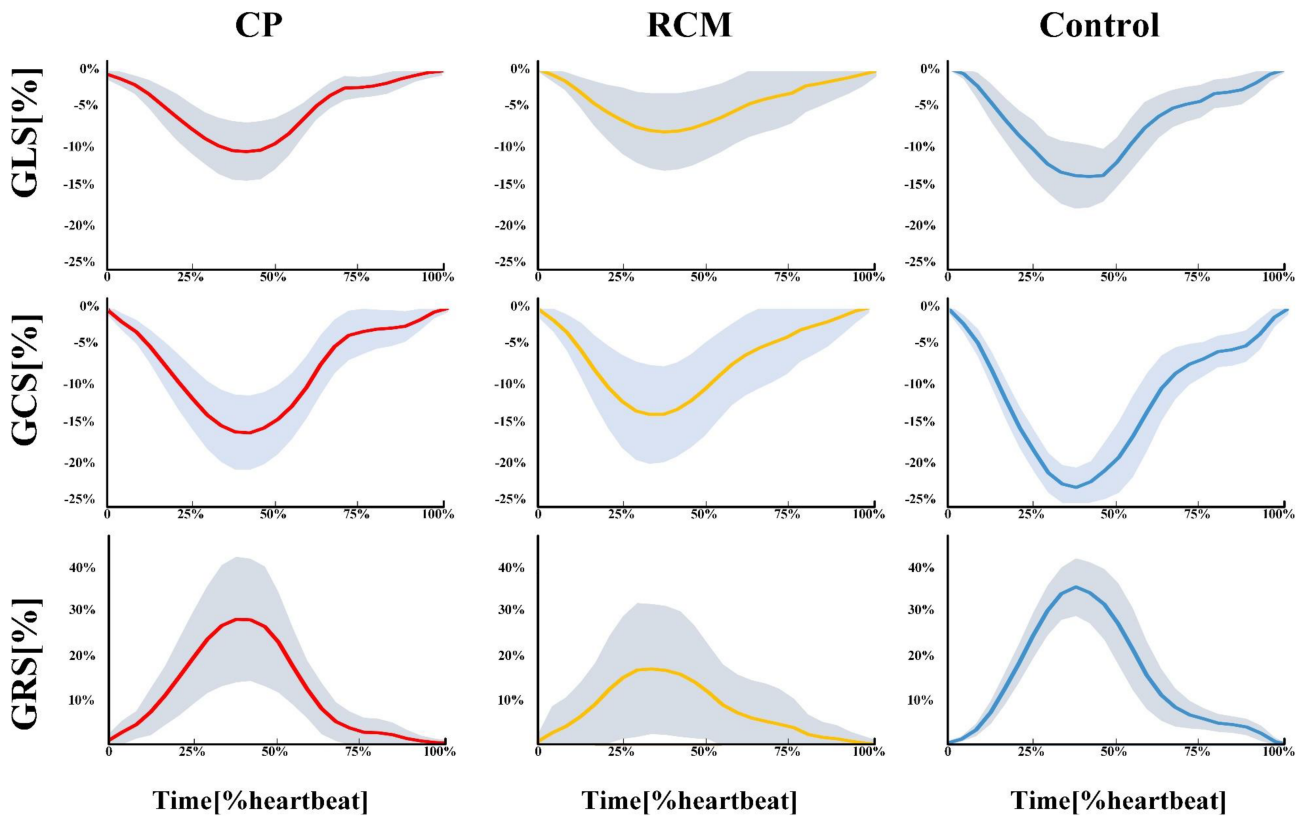
circumferential directions, but not in the radial direction. The pattern of CP corresponded to the characteristic 'plateau' pattern, that is, a rapid down and plateau of the time–strain curves from peak global strain (start of diastole) to passive filling, followed by slowing down towards the baseline at the end of diastole. The steady plateau appeared approximately in the middle and later half of the diastolic period. The pattern of RCM corresponded to the slow and steady gradual decline of the time–strain curves towards the baseline during the whole diastolic period. The pattern of the control group corresponded to a rapid decrease of the start of diastole towards the baseline with a temporary rapid down at the end of diastole.

Upon comparing the LV time–strain curve patterns of the CP, RCM, and control groups in the same directions (*Figure 3*), we found that the peak strain of the control group was the largest, followed by the CP and RCM groups. In the longitudinal and circumferential directions, the characteristic 'plateau' pattern of time–strain curves could be seen in the CP but not in the RCM during the diastolic period. At the end of diastole, the most rapid decline towards the baseline was seen in the control group, followed by the CP and RCM groups. Furthermore, the characteristic time–strain curves of the CP and RCM groups showed similar characteristics in CMR-FT and STE. The characteristic 'plateau' pattern of the time–strain curve was specific for CP but not RCM and could also be duplicated by STE. The time–strain curves and bull's-eye plots of CP and RCM derived from CMR-FT and STE of the same patients are shown in *Figure* 4A,B.

The global strain ratio of 0–50%/50–75% diastolic period and 50–75%/75–100% diastolic period

We divided the whole diastolic period (from peak strain to end-diastole) into 50%, 75%, and 100% diastolic periods, and gained the global strain of 0–50%, 50–75%, and 75–100% diastolic period in the CP, RCM, and control groups. We found

that in the circumferential direction, CP and RCM showed significant differences in the global strain ratios of the 0–50%/50–75% and 50–75%/75–100% diastolic periods. The GCS ratio of the 0–50%/50–75% diastolic period in the CP group was higher than that of the RCM group [CP vs. RCM: 17.01 (8.67, 23.75) vs. 5.38 (1.93, 11.24), *P* = 0.001], while the GCS ratio of the 50–75%/75–100% diastolic period of the CP group was lower than that of the RCM group [CP vs. RCM: 0.36 (0.15, 1.67) vs. 1.12 (0.70, 5.58), *P* < 0.001] (*Table 3*).

Diagnostic performance of left ventricular myocardial deformation parameters

The diagnosis value for peak global strain, strain ratio of LW/SW, and strain ratios of 0–50%/50–75% and 50–75%/75–100% diastolic periods to distinguish between CP and RCM are summarized in *Table 4*. The area under the receiver-operating characteristic (AUC) curve was significantly greater for the peak GLS (AUC = 0.78; *P* < 0.001) and the GCS ratio of 0–50%/50–75% diastolic period (AUC = 0.78; *P* < 0.001) than for the other parameters. The cut-off value of peak GLS was −9.15% (sensitivity, 85%; specificity, 78%) and that for the GCS ratio of the 0–50%/50–75% diastolic period was 7.27 (sensitivity, 88%; specificity, 73%).

Discussion

To our knowledge, we not only probed the dissimilarities of LV global and segmental myocardial deformation but also proposed the characteristic differences of LV time–strain curve patterns between CP and RCM for the first time. The results of our study can be summarized as follows: (i) the peak GLS and GCS of RCM were significantly lower than CP, which had significant differential diagnosis value; (ii) the GCS and GRS ratios of LW/SW of the basal segment of CP

Figure 3 LV time–strain curve patterns of the CP, RCM, and control groups. The blue line, red line, and yellow line represent the time–strain curve patterns of the control group, CP group, and RCM group, respectively. The black line represents the electrocardiography pattern. The arrowhead shows how the peak strain sequentially lessened from normal control group to the CP group and the RCM group in longitudinal, circumferential, and radial directions. The dotted line (A) indicates the first inflection point, as the end of rapid filling/beginning of passive filling. The dotted line (B) indicates the second inflection point, as the atrial contraction. Between dotted line (A) and dotted line (B), the characteristic 'plateau' can be seen in the longitudinal and circumferential directions of the CP, but not in the RCM. CP, constrictive pericarditis; RCM, restrictive cardiomyopathy; GLS, global longitudinal strain; GCS global circumferential strain; GRS, global radial strain; LV, left ventricle.
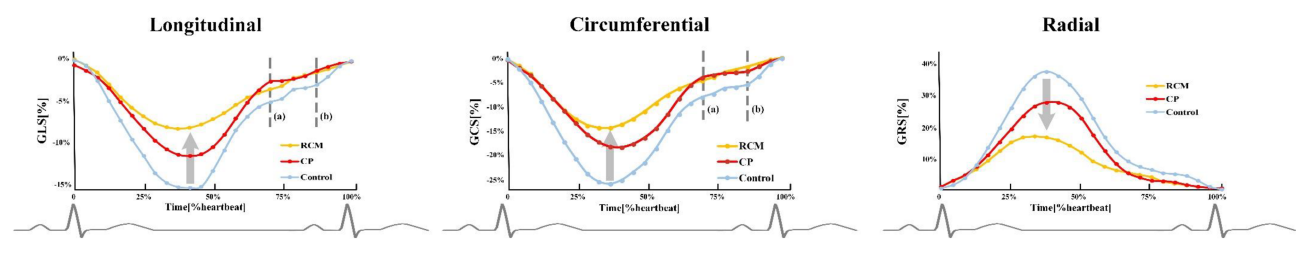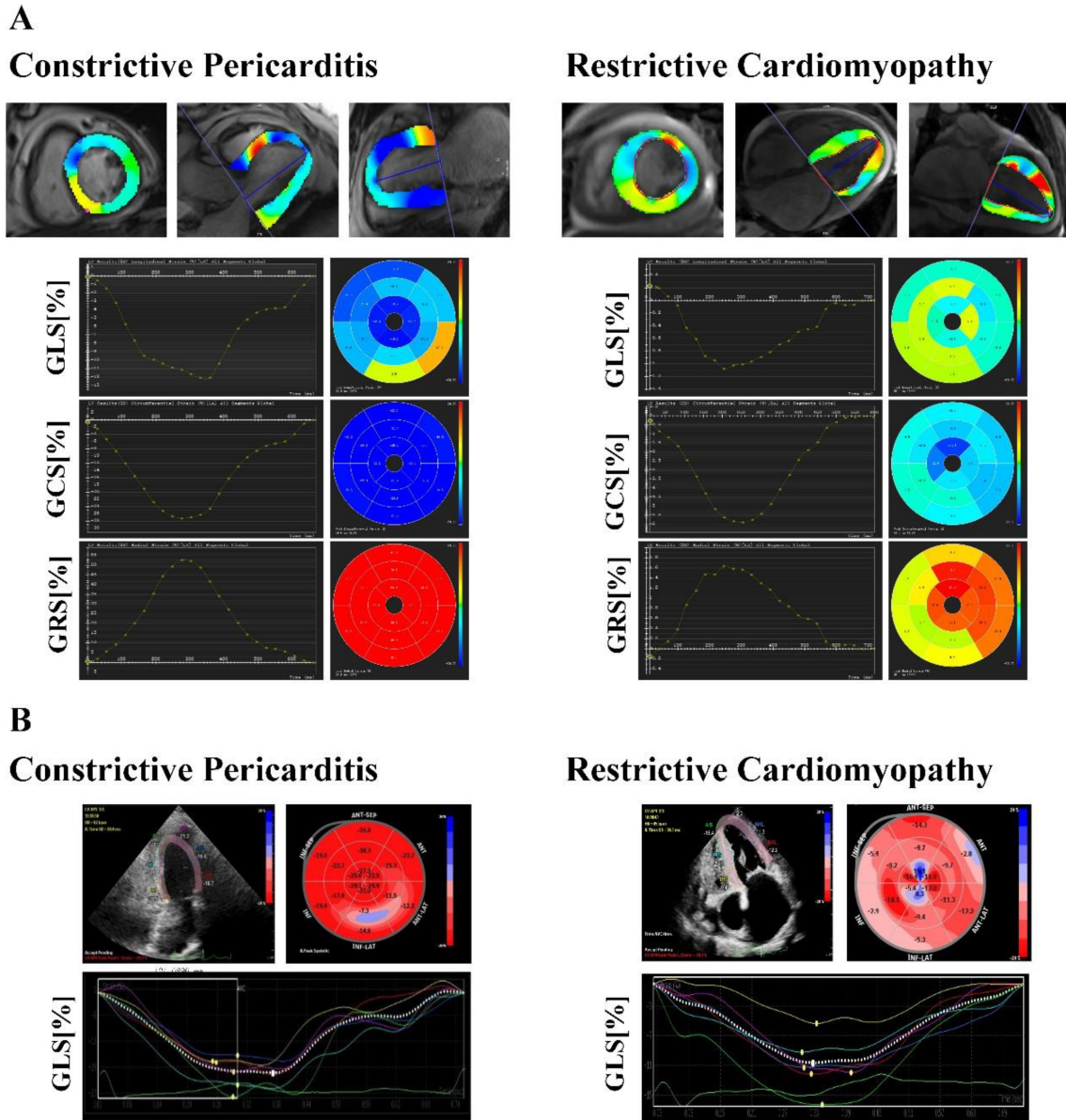
Figure 4 (A) CMR-FT and (B) STE-derived time–strain curves and bull's-eye plots from the same patient. CMR-FT, cardiac magnetic feature tracking; GCS global circumferential strain; GLS, global longitudinal strain; GRS, global radial strain; STE, speckle-tracking echocardiography.

were lower than RCM, which had significant diagnostic value in distinguishing between CP and RCM; (iii) during the diastolic period, the characteristic 'plateau' patterns of the time–strain curve appeared in the longitudinal and circumferential directions of CP but not the RCM group; (iv) the GCS ratio of the 0–50%/50–75% diastolic period of the CP group was higher than that of the RCM, while the GCS ratio of the 50–75%/75–100% diastolic period of the CP group was lower than that of the RCM group.

In our study, the peak GLS, GCS, and GRS of the CP and RCM groups were lower than those of the control group. This is because in the process of diastolic filling, LV stiffness and peri-cardial restraint will lead to increased LV afterload and impaired systolic function, which ultimately leads to weaker myocardial deformation and lower peak global strain.[17,18] Furthermore, the peak GLS and GCS of the RCM group were significantly lower than those of the CP group. Unlike the impaired left ventricular compliance caused by internal myocardial stiffness in RCM, the impaired left ventricular compliance in CP was caused by external pericardial restraint. Therefore, CP will retain part of the normal myocardial contraction and relaxation function,[19,20] and the global strain of CP compared with RCM will be relatively retained. On the other hand, longitudinal deformation, presented as GLS, contributes to

Table 3 The global strain ratio of 0–50%/50–75% diastolic period and 50–75%/75–100% diastolic period

	CP (n = 32)	RCM (n = 27)	Control (n = 25)	H value	P value
The ratio of 0–50%/50–75% diastolic period					
GLS	6.29 (4.71, 19.76)	5.25 (2.77, 8.45)*	10.32 (6.33, 23.08)	8.381	0.015
GCS	17.01 (8.67, 23.75)#	5.38 (1.93, 11.24)*	12.77 (6.95, 26.64)	15.173	0.001
GRS	8.75 (4.51, 19.36)	12.21 (4.81, 22.02)	14.44 (7.38, 54.42)	3.444	0.179
The ratio of 50–75%/75–100% diastolic period					
GLS	1.62 (0.36, 50.45)	1.08 (0.51, 4.02)	0.76 (0.27, 1.57)	4.210	0.122
GCS	0.36 (0.15, 1.67)#	1.12 (0.70, 5.58)*	0.22 (0.13, 0.53)	17.562	<0.001
GRS	1.88 (0.69, 16.97)†	5.35 (0.66, 70.54)*	0.74 (0.18, 1.19)	13.354	0.001

CP, constrictive pericarditis; GCS global circumferential strain; GLS, global longitudinal strain; GRS, global radial strain; RCM, restrictive cardiomyopathy.
Continuous variables are presented as mean ± SD or median (interquartile range).
#$P < 0.05$ CP vs. RCM.
†$P < 0.05$ CP vs. control.
*$P < 0.05$ RCM vs. control.

Table 4 The diagnosis value of global strain and strain ratio in distinguishing CP and RCM

	AUC	P value	Cut-off value	Sensitivity (%)	Specificity (%)
Peak GLS (%)	0.78	<0.001	−9.15%	85%	78%
Peak GCS (%)	0.69	0.012	−18.25%	85%	50%
The GCS ratio of LW/SW					
Basal	0.69	0.014	1.17	82%	75%
Mid	0.52	0.761			
The GRS ratio of LW/SW					
Basal	0.68	<0.001	1.39	67%	78%
Mid	0.54	0.616			
The GCS ratio of 0–50%/50–75% diastolic period	0.78	<0.001	7.27	88%	73%
The GCS ratio of 50–75%/75–100% diastolic period	0.70	0.008	0.54	85%	63%

AUC, area under the receiver-operating characteristic curve; CP, constrictive pericarditis; GCS global circumferential strain; GLS, global longitudinal strain; GRS, global radial strain; LW/SW, lateral/septal wall; RCM, restrictive cardiomyopathy.

shortening of subendocardial myofibres. Circumferential deformation, presented as GCS, reflects subepicardial myofibres.[21,22] The peak GLS and GCS that are mainly manifested as LV rotation, twist, or torsion, and are able to detect the slightly impaired systolic function with preserved LVEF, have significant differential diagnosis value between CP and RCM.

Previous studies have raised the question of whether there was a difference in the strain ratio of LV lateral/septal wall between CP and RCM.[11,14] The LV lateral wall of CP was considered to show regional constraint and the septal wall was thought to be free and unaffected by calcification; however, both the lateral and septal walls of RCM showed myocardial stiffness and had no significant difference with respect to each other. Our study systematically analysed the strain ratios of LW/SW in different directions and segments. It was found that the LW/SW strain ratios in the circumferential and radial directions of the CP base segment were lower than that of the RCM. We verified the above point of view and believed that the most common part of LV calcification and adhesion was the atrioventricular groove of the basal segment of CP.[23,24] In addition, the main involvement of CP was subepicardial fibre dysfunction, and even transmural fibre dysfunction, which eventually led to a decrease in GCS and GRS of the lateral wall.[25]

The LV time–strain curve patterns of CP and RCM, which described their LV contraction and relaxation process showed characteristic differences. Patients with CP were inhibited by external pericardial restraint, but this hardly impaired the elastic properties of the internal myocardium itself; rather, it retained parts of the normal myocardial relaxation function in early diastole. From early diastolic filling to the end of rapid filling, the LV filling pressure and LV global strain of CP patients with almost normal myocardial relaxation function showed a rapid decrease. Further, a rapid decrease of the time–strain curves from the start of diastole to passive filling could be seen in the CP pattern, similar to the control group. In the passive filling period, owing to continued inertial effects, the LV chamber filled negatively and LV global strain decreased slowly.[26] Furthermore, due to the suppression of thickening and calcification of the pericardium and adhesion of the pericardial visceral layer and wall layer, the LV filling process was prolonged, and the decrease of LV global strain was more stagnant than in the RCM and control groups. The characteristic 'plateau' of CP time–strain curve pattern could be seen in middle diastole. At the end of diastole, the LA contraction and rapid LV filling made a transient rapid decrease of LV global strain and a transient rapid decrease in LV time–strain curve pattern of the control group. However, the end-diastolic ventricular relaxation function was impaired in

CP patients affected by the pericardial restraint, which led to prolonged LV filling, slowed blood flow from the LV into the systemic circulation, and increased LA afterload.[27] Eventually, the characteristic 'plateau' of the LV time–strain curve pattern of CP was extended and a down towards the baseline was slower than that of the control group at the end of diastole. We also found that the characteristic steady 'plateau' of CP was characterized by tiny fluctuations <5% in the middle and latter half of the diastolic period, and appeared at the 50–75% diastolic period of CP, but not in RCM. The global strain of 50–75% diastolic period of CP was extremely small (approximately equal to 0). Therefore, the global strain ratio of 0–50%/50–75% diastolic period of the CP group was higher than that of the RCM group, while the global strain ratio of the 50–75%/75–100% diastolic period of the CP group was lower than that of the RCM group.

In the RCM group, the abnormal elastic properties of the myocardium and intercellular matrix and interstitial fibrosis led to myocyte apoptosis, degeneration, and LV chamber stiffness.[28] All of these led to irreversibly impaired myocardial function, further prolonged relaxation, reduced effective operative compliance of the LV, and increased LV pressure.[3] From the early diastole to the end diastole, the ventricular diastolic function of RCM was impaired, and the diastolic process was gradually delayed. The time–strain curve pattern of RCM corresponded to the slow and steady gradual decline towards the baseline during the whole diastolic period.

Limitations

The major limitation of this study is lack of invasive haemodynamic data for further diagnostic information, which poses a limitation to the true sensitivity and specificity of the CMR-FT findings for the differential diagnosis of CP and RCM. We will include more CP and RCM patients diagnosed by right heart catheterization in the future studies. Second, the study population was relatively small, and myocardial amyloidosis was the main part of RCM patients, which might limit the generalizability of these results. We plan to further expand the study population and collaborate with multiple research centres. Third, some studies have confirmed the accuracy and repeatability between CMR-FT and STE. We will further explore the consistency and repeatability of the LV time–strain curve patterns of CP and RCM derived from different tissue-tracking technologies to verify the reliability of LV time–strain curve patterns for differentiating CP from RCM patients. Finally, a long-term follow-up study would be very useful in the future to assess the relationship between the prognosis relevance and the characteristic time–strain curve patterns changes of CP and RCM.

Conclusions

The CMR-FT can identify three different characteristic LV time–strain curve patterns in CP, RCM, and healthy control subjects and quantify the myocardial deformation in each group. Each time–strain curve pattern is associated with different haemodynamic conditions and contraction and relaxation functions and provides a novel and simplified way to differentiate CP from RCM. The characteristic 'plateau' pattern of the time–strain curve is specific for CP and not RCM, and this curve can also be duplicated by STE.

Acknowledgements

Conflict of interest

None declared.

Funding

References

1. Pereira NL, Grogan M, Dec GW. Spectrum of restrictive and infiltrative cardiomyopathies: Part 1 of a 2—part series. *J Am Coll Cardiol* 2018; **71**: 1130–1148.

2. Garcia MJ. Constrictive pericarditis versus restrictive cardiomyopathy? *J Am Coll Cardiol* 2016; **67**: 2061–2076.

3. Nishimura RA, Borlaug BA. Diastology for the clinician. *J Cardiol* 2019; **73**: 445–452.

4. Szabo G, Schmack B, Bulut C, Soos P, Weymann A, Stadtfeld S, Karck M. Constrictive pericarditis: risks, aetiologies and outcomes after total pericardiectomy: 24 years of experience. *Eur J Cardiothorac Surg* 2013; **44**: 1023–1028 discussion 1028.

5. Ho G, Peng E, Hermuzi A, Hasan A. Restrictive cardiomyopathy or constrictive pericarditis: an unresolved conundrum. *World J Pediatr Congenit Heart Surg* 2018; **9**: 360–363.

6. Oh JKHL, Seward JB, Danielson GK. Diagnostic role of Doppler echocardiography in constrictive pericarditis. *J Am Coll Cardiol* 1994; **23**: 154–162.

7. Ha JW, Oh JK, Ommen SR, Ling LH, Tajik AJ. Diagnostic value of mitral annular velocity for constrictive pericarditis in the absence of respiratory variation in mitral inflow velocity. *J Am Soc Echocardiogr* 2002; **15**: 1468–1471.

8. Talreja DR, Edwards WD, Danielson GK, Schaff HV, Tajik AJ, Tazelaar HD, Breen JF, Oh JK. Constrictive pericarditis in 26 patients with histologically normal pericardial thickness. *Circulation* 2003; **108**: 1852–1857.

9. Thalen S, Maanja M, Sigfridsson A, Maret E, Sorensson P, Ugander M. The dynamics of extracellular gadolinium-based contrast agent excretion into pleural and pericardial effusions quantified by T1 mapping cardiovascular magnetic resonance. *J Cardiovasc Magn Reson* 2019; **21**: 71.

10. Kanagala P, Cheng ASH, Singh A, McAdam J, Marsh AM, Arnold JR, Squire IB, Ng LL, McCann GP. Diagnostic and prognostic utility of cardiovascular magnetic resonance imaging in heart failure with preserved ejection fraction—implications for clinical trials. *J Cardiovasc Magn Reson* 2018; **20**: 1–12.

11. Amaki M, Savino J, Ain DL, Sanz J, Pedrizzetti G, Kulkarni H, Narula J, Sengupta PP. Diagnostic concordance of echocardiography and cardiac magnetic resonance-based tissue tracking for differentiating constrictive pericarditis from restrictive cardiomyopathy. *Circ Cardiovasc Imaging* 2014; **7**: 819–827.

12. Sengupta PP, Krishnamoorthy VK, Abhayaratna WP, Korinek J, Belohlavek M, Sundt TM 3rd, Chandrasekaran K, Mookadam F, Seward JB, Tajik AJ. Disparate patterns of left ventricular mechanics differentiate constrictive pericarditis from restrictive cardiomyopathy. *JACC Cardiovasc Imaging* 2008; **1**: 29–38.

13. Nucci EM, Lisi M, Cameli M, Baldi L, Puccetti L, Mondillo S, Favilli R, Lunghetti S. The role of 3D and speckle tracking echocardiography in cardiac

amyloidosis: a case report. *Eur Rev Med Pharmacol Sci* 2014; **18**: 74–77.

14. Kusunose K, Dahiya A, Popovic ZB, Motoki H, Alraies MC, Zurick AO, Bolen MA, Kwon DH, Flamm SD, Klein AL. Biventricular mechanics in constrictive pericarditis comparison with restrictive cardiomyopathy and impact of pericardiectomy. *Circ Cardiovasc Imaging* 2013; **6**: 399–406.

15. Hurrell DG, Nishimura RA, Higano ST, Appleton CP, Danielson GK, Holmes DR Jr, Tajik AJ. Value of dynamic respiratory changes in left and right ventricular pressures for the diagnosis of constrictive pericarditis. *Circulation* 1996; **93**: 2007–2013.

16. Lang RM, Badano LP, Mor-Avi V, Afilalo J, Armstrong A, Ernande L, Flachskampf FA, Foster E, Goldstein SA, Kuznetsova T, Lancellotti P, Muraru D, Picard MH, Rietzschel ER, Rudski L, Spencer KT, Tsang W, Voigt JU. Recommendations for cardiac chamber quantification by echocardiography in adults: an update from the American Society of Echocardiography and the European Association of Cardiovascular Imaging. *J Am Soc Echocardiogr* 2015; **28**: 1–39 e14.

17. Kosmala W, Rojek A, Przewlocka-Kosmala M, Mysiak A, Karolko B, Marwick TH. Contributions of nondiastolic factors to exercise intolerance in heart failure with preserved ejection fraction. *J Am Coll Cardiol* 2016; **67**: 659–670.

18. Huang W, Chai SC, Lee SGS, MacDonald MR, Leong KTG. Prognostic factors after index hospitalization for heart failure with preserved ejection fraction. *Am J Cardiol* 2017; **119**: 2017–2020.

19. Rajagopalan N, Garcia MJ, Rodriguez L, Murray RD, Hansen CA, Stugaard M, Thomas JD, Klein AL. Comparison of new Doppler echocardiographic methods to differentiate constrictive pericardial heart disease and restrictive cardiomyopathy. *Am J Cardiol* 2001; **87**: 86–94.

20. Palka P, Lange A, Donnelly JE, Nihoyannopoulos P. Differentiation be-

tween restrictive cardiomyopathy and constrictive pericarditis by early diastolic Doppler myocardial velocity gradient at the posterior wall. *Circulation* 2000; **102**: 655–662.

21. Voigt JU, Cvijic M. 2- and 3-dimensional myocardial strain in cardiac health and disease. *JACC Cardiovasc Imaging* 2019; **12**: 1849–1863.

22. Duncan AE, Alfirevic A, Sessler DI, Popovic ZB, Thomas JD. Perioperative assessment of myocardial deformation. *Anesth Analg* 2014; **118**: 525–544.

23. O'Leary SM, Williams PL, Williams MP, Edwards AJ, Roobottom CA, Morgan-Hughes GJ, Manghat NE. Imaging the pericardium: appearances on ECG-gated 64-detector row cardiac computed tomography. *Br J Radiol* 2010; **83**: 194–205.

24. Choi JH, Choi JO, Ryu DR, Lee SC, Park SW, Choe YH, Oh JK. Mitral and tricuspid annular velocities in constrictive pericarditis and restrictive cardiomyopathy: correlation with pericardial thickness on computed tomography. *JACC Cardiovasc Imaging* 2011; **4**: 567–575.

25. Claus P, Omar AMS, Pedrizzetti G, Sengupta PP, Nagel E. Tissue tracking technology for assessing cardiac mechanics: principles, normal values, and clinical applications. *JACC Cardiovasc Imaging* 2015; **8**: 1444–1460.

26. Redfield MM, Solomon CG. Heart failure with preserved ejection fraction. *New Engl J Med* 2016; **375**: 1868–1877.

27. Liu S, Ma C, Ren W, Zhang J, Li N, Yang J, Zhang Y, Qiao W. Regional left atrial function differentiation in patients with constrictive pericarditis and restrictive cardiomyopathy: a study using speckle tracking echocardiography. *Int J Cardiovasc Imaging* 2015; **31**: 1529–1536.

28. Rammos A, Meladinis V, Vovas G, Patsouras D. Restrictive cardiomyopathies: the importance of non-invasive cardiac imaging modalities in diagnosis and treatment—a systematic review. *Radiol Res Pract* 2017; **2017**: 2874902.